



Kent Academic Repository

Pickup, David M., Sowrey, Frank E., Skipper, Laura J., Newport, Robert J., Gunawidjaja, Philips N., Drake, Kieran O., Smith, Mark E., Saravanapavan, Priya and Hench, Larry L. (2005) *The structure of TiO₂-SiO₂ and CaO-SiO₂ sol-gel glasses from neutron diffraction and solid state NMR using isotopic enrichment of titanium, calcium and oxygen*. *Physics and Chemistry of Glasses*, 46 (4). pp. 433-438. ISSN 0031-9090.

Downloaded from

<https://kar.kent.ac.uk/8225/> The University of Kent's Academic Repository KAR

The version of record is available from

<http://www.ingentaconnect.com/content/sgt/pcg/2005/00000046/00000004/art00023>

This document version

UNSPECIFIED

DOI for this version

Licence for this version

UNSPECIFIED

Additional information

Versions of research works

Versions of Record

If this version is the version of record, it is the same as the published version available on the publisher's web site. Cite as the published version.

Author Accepted Manuscripts

If this document is identified as the Author Accepted Manuscript it is the version after peer review but before type setting, copy editing or publisher branding. Cite as Surname, Initial. (Year) 'Title of article'. To be published in *Title of Journal*, Volume and issue numbers [peer-reviewed accepted version]. Available at: DOI or URL (Accessed: date).

Enquiries

If you have questions about this document contact ResearchSupport@kent.ac.uk. Please include the URL of the record in KAR. If you believe that your, or a third party's rights have been compromised through this document please see our [Take Down policy](https://www.kent.ac.uk/guides/kar-the-kent-academic-repository#policies) (available from <https://www.kent.ac.uk/guides/kar-the-kent-academic-repository#policies>).

The structure of $\text{TiO}_2\text{--SiO}_2$ and CaO--SiO_2 sol-gel glasses from neutron diffraction and solid state NMR using isotopic enrichment of titanium, calcium and oxygen

D. M. Pickup, F. E. Sowrey, L. J. Skipper, R. J. Newport¹

School of Physical Sciences, University of Kent, Canterbury, CT2 7NH, UK

P. Gunawidjaja, K. O. Drake, M. E. Smith

Department of Physics, University of Warwick, Coventry, CV4 7AL, UK

P. Saravanapavan & L. L. Hench

Department of Materials, Imperial College London, London, SW7 2AZ, UK

Manuscript received 18 August 2004
Accepted 22 December 2004

An advanced materials characterisation methodology has been used to examine systematically a range of sol-gel glass materials of contemporary interest. Neutron diffraction using ^{46}Ti and ^{48}Ti stable isotopes, and isotope-enriched ^{17}O MAS NMR, have been used to characterise the structure of catalytically active $(\text{TiO}_2)_x(\text{SiO}_2)_{1-x}$ sol-gel glass as a function of calcination temperature ($T=250, 500$ and 750°C). The results reveal directly two Ti–O distances in a homogeneous $(\text{TiO}_2)_{0.18}(\text{SiO}_2)_{0.82}$ sol-gel derived glass. The detailed nature of the Ti environment may be discerned from a combination of neutron scattering data with solid state NMR, including the possible presence of phase separation at the higher temperature. Neutron diffraction using ^{44}Ca , and isotope enriched ^{17}O MAS NMR have also been used to study the detailed nature of the structure of CaO--SiO_2 bioactive sol-gel glasses. The results offer a direct observation of multiple Ca–O distances in this material, and pave the way to a fuller understanding of the role of Ca in its bioactivity. The results presented here are consistent with, but greatly extend our previous XRD, ^{17}O and ^{29}Si MAS-NMR, XANES and EXAFS studies of these materials.

An essential step in achieving an understanding of why amorphous materials exhibit the properties they do is gaining a full knowledge of the atomic scale structure of such materials. For instance, titania–silica mixed oxide glasses, $(\text{TiO}_2)_x(\text{SiO}_2)_{1-x}$, have found use as ultra low thermal expansion glasses⁽¹⁾ and thin films with tailored refractive indices.⁽²⁾ However, the majority of

the recent work on the titania–silica system focuses on its catalytic properties,^(3–5) and in particular on how these are related to the local environment of titanium in the structure.

Similarly, to allow people to remain active, and to contribute to society for longer, the need for new materials to replace and repair worn out and damaged tissues becomes ever more important^(6–9). Melt quenched silicate glasses containing calcium and phosphorus, and often alkali metals, have been much studied for their applications to promote bone regeneration and to fuse to living bone. More recent work has focused on the use of the relatively low temperature sol-gel route for generating bioactive glasses, by which fewer components are required and a wider spectrum of compositions and glass porosities may be achieved. Samples of the general formula $(\text{CaO})_x(\text{SiO}_2)_{1-x}$ have been shown to possess significant potential as bioactive bone regenerative materials.^(10,11)

Titania–silica

There have been several structural studies on $(\text{TiO}_2)_x(\text{SiO}_2)_{1-x}$ sol-gel glasses focusing both on the titanium environment and on the degree of phase separation between the oxide components. Dirken *et al.*⁽¹²⁾ demonstrated that ^{17}O NMR is a powerful technique for observing phase separation in such systems. Extended x-ray absorption fine structure (EXAFS), has been used to directly probe the titanium environment. Anderson *et al.*⁽¹³⁾ used EXAFS to measure the Ti–O bond distance in gels containing 8, 18 and 41 mol% Ti. The results indicated an increase in the average Ti–O bond distance from 1.8 to 1.9 Å with increasing titanium content from 8 to 41 mol%; this change was attributed

¹ Corresponding author. Email address: r.j.newport@kent.ac.uk

to the titanium environment changing from substituted within the silica network to phase separated into domains of TiO_2 . Rigden *et al*⁽¹⁴⁾ used neutron and x-ray diffraction to study a similar set of samples and, on the basis of a measured Ti-O bond distance of ~ 1.8 Å, reached the conclusion that titanium predominantly substitutes for silicon within the glass network. Despite the value of this study, the limited resolution of the x-ray data and the problem with overlapping correlations in the pair distribution function obtained from the neutron data precluded a full analysis of the titanium site. One of the most useful techniques for studying titanium containing oxides is XANES, which indirectly yields information on the titanium environment from the shape of the Ti K-edge x-ray absorption profile and can distinguish between tetrahedral and octahedral coordinated titanium (TiO_4 and TiO_6 , respectively, hereafter).⁽¹⁵⁾ Mountjoy *et al*⁽¹⁶⁾ exploited this technique to confirm two important structural trends that occur in $(\text{TiO}_2)_x(\text{SiO}_2)_{1-x}$ materials. Firstly, as the composition is varied from $x=0.08$ – 0.41 there is a corresponding increase in the number of TiO_6 sites. Secondly, a clear correlation was established between the abundance of TiO_4 sites and the temperature of the heat treatment used in the gel-to-glass processing. More recently, the XANES technique was taken further and applied to samples that were heated *in situ* to temperatures of up to 250°C .^(17,18) Both these studies revealed the existence of TiO_6 sites which could be reversibly converted to TiO_4 sites upon heating to 150 – 250°C .

Despite the many studies outlined above, the exact nature of the titanium site has never been fully characterised. Here, for the first time, we combine two advanced structural probes in the study of this class of material: neutron diffraction with isotopic substitution (NDIS) can provide unambiguous and quantitative information on the Ti environment, whilst ^{17}O MAS NMR can directly probe this structural location.

Calcium-silica

The exact mechanism by which calcium-silica materials promote bone growth and the requirements for optimisation of their properties are still as yet only partially understood, but have been strongly linked to the evident ease of calcium dissolution from the glass matrix.⁽¹¹⁾ A great deal of interest in the structure of these materials has therefore been engendered, especially the nature and the role of the Ca sites within the glass network.

The local calcium environment in crystalline calcium silicate minerals and apatites is extremely diverse; in most minerals there are several crystallographically distinct Ca environments. This diversity adds to the complexity of the Ca environment and ensures a wide range of possible calcium-oxygen coordination numbers. Amorphous materials are intrinsically even more structurally complex in the sense that the long-range order of the crystalline form is lost. Analysis of the short range environment in calcium silicate glasses has been attempted using x-ray absorption fine structure and near edge structure (EXAFS and XANES)⁽¹⁹⁾ and by x-ray powder diffraction,⁽²⁰⁾ however the complexity of the calcium environment limits the useful information available from these techniques. For instance, conventional diffraction measurements show the Ca-O correlations as a broad feature centred around 2.35 Å, but this feature is overlapped by the strong O-O correlation making a quantitative measure of Ca environment impossible based solely on such data.

Experimental method

Sample preparation

Initially, samples of natural TiO_2 , $^{46}\text{TiO}_2$ (72.1 atom% enriched, Isoflex USA), $^{48}\text{TiO}_2$ (99.8 at% enriched, CK Gas Products) and $^{48/49}\text{TiO}_2$ (74.3 and 23.9 at% enriched respectively, CK Gas Products and Isoflex USA) were converted to the corresponding isopropoxides via their chloride analogues. The $(\text{TiO}_2)_x(\text{SiO}_2)_{1-x}$ sol-gels, with x nominally 18 mol%, were prepared by reacting the isotopically enriched $\text{Ti}(\text{OPr})_4$ with TEOS (tetraethyl orthosilicate, $\text{Si}(\text{OEt})_4$) in the presence of H_2O and HCl using the procedure described previously.⁽²¹⁾ In the case of the samples for the NMR study, 45 at% ^{17}O -enriched water was used. Samples were heated to 250, 500 and 750°C at a ramp rate of 5°Cmin^{-1} under an atmosphere of flowing air; each temperature was maintained for 2 h. Sample details are shown in Table 1.

Two samples of $(\text{CaO})_{0.3}(\text{SiO}_2)_{0.7}$ were prepared samples were prepared following previously published procedures,^(22,23) one containing natural Ca and the other ^{44}Ca . Sample details are shown in Table 1.

Neutron diffraction and NMR

Diffraction methods give access to both short and medium range order (up to ~ 15 Å). However, for multicomponent systems, the overlapping of coordination shells limits the structural information which can be extracted from the data. NDIS allows the separation

Table 1. Sample characterisation of heat treated $(\text{TiO}_2)_x(\text{SiO}_2)_{1-x}$ sol-gel glasses containing natural titanium and of $(\text{CaO})_x(\text{SiO}_2)_{1-x}$ sol-gel bioactive glasses containing natural calcium

Sample (notional mol% & heat treatment temperature)	Composition (atm%)						$c_{\text{Ti}}/(c_{\text{Ti}}+c_{\text{Si}})$	Density (g/cm^3)
	Ti	Si	O	C	H			
$\text{Ti}, x=0.18$ 250°C	3.4	16.1	56.3	2.9	21.4	0.17	0.17	2.23(5)
$\text{Ti}, x=0.18$ 500°C	4.4	20.7	62.9	0.00	12.1	0.17	0.17	2.27(2)
$\text{Ti}, x=0.18$ 750°C	4.4	21.4	61.3	0.00	12.9	0.17	0.17	2.36(2)
	Ca	Si	O		H			
Ca, 600°C	12.2	21.0	54.4		12.4			2.21(2)

of the partial pair distribution functions associated with one specific element in the sample.⁽²⁴⁾ Using this technique, it is possible to characterise fully the coordination environment of the isotopically substituted element as well as determining its relationship to the glass network. Until now, there have been no NDIS studies on sol-gel prepared materials, probably due to the complexity of enriching the precursor reagents and the difficulty in preparing two sol-gel samples that do not differ significantly in structure or composition except for the isotopic substitution.

The initial stage of analysis of neutron diffraction data from an amorphous material entails the removal of background scattering, correction for absorption and multiple scattering and subtraction of the self scattering term. The resultant scattered intensity, $i(Q)$, where $Q=4\pi\sin\theta/\lambda$, can reveal structural information by Fourier transformation to obtain the total correlation function⁽²⁶⁾

$$T(r) = T^0(r) + \frac{2}{\pi} \int_0^\infty Q i(Q) M(Q) \sin(Qr) d(Q) \quad (1)$$

where $T^0(r) = 4\pi r \rho^0 (\sum_i c_i b_i)^2$ is the average density contribution (ρ^0 is the macroscopic number density, and c_i and b_i are the atomic fraction and coherent scattering length, respectively, of element i), and $M(Q)$ is a modification function used to take into account the maximum experimentally attainable value of Q .

If two experiments are performed in which the scattering length of element A is varied (by isotopic substitution), the difference between the experimental correlation functions is of the form⁽²⁹⁾

$$\Delta T(r) = T(r) - T'(r) = c_A^2 (b_A^2 - b_{A'}^2) t'_{AA}(r) + 2 \sum_{j \neq A} c_A c_j b_j (b_A - b_{A'}) t'_{Aj}(r) \quad (2)$$

where $t'_{AX}(r)$ represents the partial pair correlation function for elements A and X . Thus, only the structural environment of element A is probed.

Structural information can be obtained from the neutron diffraction data by modelling the Q -space data and converting the results to r -space by Fourier transformation to allow comparison with the experimentally determined correlation function.⁽²⁷⁾ The neutron scattering lengths are as follows: ^{46}Ti , $b=2.469$ fm, ^{48}Ti , $b=-6.063$ fm and ^{nat}Ti , $b=-3.438$ fm (it should be noted that the negative scattering lengths arise from a π phase shift of the neutron wavefunction on scattering). For the two calcia-silica samples: ^{44}Ca , $b=1.42$ fm, and for ^{nat}Ca , $b=4.70$ fm.

The neutron diffraction data presented here were collected on the GEM diffractometer on the ISIS spallation neutron source at the Rutherford Appleton Laboratory, UK; time-of-flight data collected over a wide range of Q (up to 50 \AA^{-1}). The ATLAS suite of programs was used to reduce and correct the data.⁽²⁵⁾

Similarly, solid state NMR is an increasingly used atomic scale, element-specific probe of the structure of materials.⁽²⁸⁾ ^{29}Si MAS NMR can determine the

network connectivity by identification of the different Q species, and the loss of organic groups and hydroxyls can be followed by ^{13}C and ^1H NMR.⁽²⁹⁾ ^{17}O on enriched samples has been shown to be extremely sensitive to the distribution of the metals through identifying the different fragments (such as $(\text{Ti,Si})\text{-O-(Si,Ti)}$) present,^(12,29) and has been used to show differences in the degree of phase separation as the functionality of the silicon precursor.⁽³⁰⁾

The ^{17}O MAS NMR spectra were collected using 4 mm MAS NMR probes (both Doty and Bruker) spinning at ~ 12 kHz on a Varian Infinity CMX-360 spectrometer, equipped with an 8.45 T magnet, operating at 48.18 MHz. Spectra were collected using θ - τ -2 θ spin-echo pulse sequences with θ corresponding to a tip angle of $\sim 90^\circ$ on the solid sample (typically 1.5 μs), τ set to the rotor period and recycle delays of 0.5–5 s, sufficient to allow relaxation. The number of co-added scans was typically 3×10^4 . Spectra were referenced to H_2O at 0 ppm.

Isotopically enriched samples of the same composition were shown to be structurally equivalent using x-ray diffraction (Station 9.1, Synchrotron Radiation Source, Daresbury Laboratory, UK). Further characterisation necessary for analysis of the neutron diffraction data was performed: elemental analysis (ICP-AES and gravimetric) was carried out by a commercial company (Medac Ltd) and in house using a Bruker S4 x-ray fluorescence spectrometer, and macroscopic densities were determined by helium pycnometry.

Results and discussion

Titania-silica

Figures 1 and 2 serve to illustrate both the method and benefit of using NDIS to study this class of materials. Figure 1(a) shows the Q -space neutron diffraction interference functions for the isotopically enriched $(\text{TiO}_2)_{0.18}(\text{SiO}_2)_{0.82}$ sol-gel glasses heated to 750°C . There are two points to note concerning these spectra.

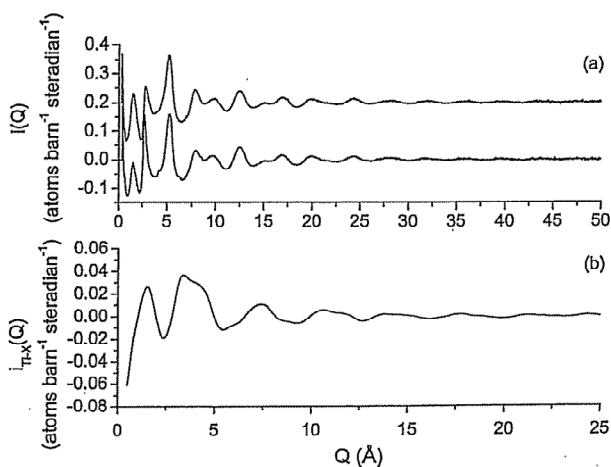


Figure 1. Typical Q -space neutron diffraction data from the isotopically enriched $(\text{TiO}_2)_x(\text{SiO}_2)_{1-x}$ sol-gel samples: (a) Q -space interference functions, $i(Q)$, from the ^{46}Ti enriched (upper trace) and ^{48}Ti enriched (lower trace) $(\text{TiO}_2)_{0.18}(\text{SiO}_2)_{0.82}$ samples heated to 750°C and (b) difference interference function obtained by subtracting the ^{46}Ti $i(Q)$ from the ^{48}Ti $i(Q)$.

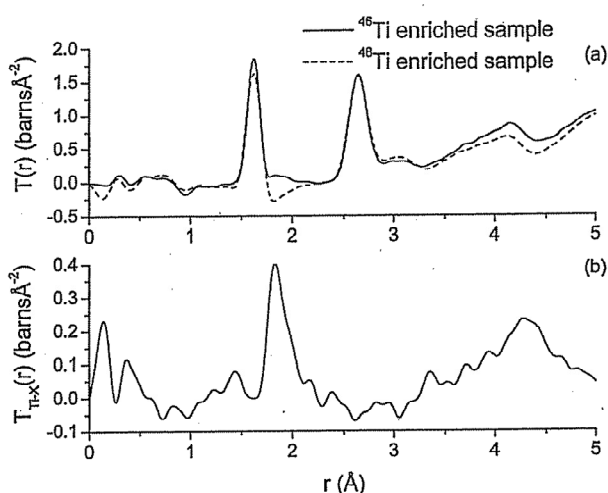


Figure 2. Real space neutron diffraction data obtained by Fourier transformation of the data shown in Figure 1: (a) total correlation functions, $T(r)$, from the ^{46}Ti enriched and ^{48}Ti enriched $(\text{TiO}_2)_{0.18}(\text{SiO}_2)_{0.82}$ samples heated to 750°C and (b) difference correlation function showing clearly a feature at just below 2 Å due to Ti-O bonding; the broad feature at $\sim 4.3\text{ Å}$ is associated with second neighbour correlations involving Ti (e.g. Ti-O-Si)

Firstly, the data are of sufficient quality over a wide range of Q ($Q_{\text{max}}=50\text{ Å}^{-1}$) to provide excellent real-space resolution when Fourier transformed. The second is to observe how similar the two spectra are. This is to be expected because the materials are mostly silica (over 80 mol%) and were prepared to be structurally equivalent: i.e. identical in all pertinent respects except for the isotope of titanium present. Figure 1(b) shows the result of subtracting the interference function of the $(^{48}\text{TiO}_2)_{0.18}(\text{SiO}_2)_{0.82}$ 750°C sample from that obtained from the ^{46}Ti -enriched sample; this difference function contains only information about the correlations involving titanium (see Equation (2)). Structural information is best observed by examining the pair distribution functions obtained by Fourier transformation of the Q -space data. Figure 2 shows the real space data obtained by Fourier transformation of the interference functions shown in Figure 1. The two $T(r)$ functions (Figure 2(a)) are dominated by peaks at ~ 1.6 and $\sim 2.6\text{ Å}$ which are assigned to the Si-O and O-O correlations, respectively. The broader feature at just over 3 Å is due to the Si-Si correlation. The information concerning the Ti-O correlation is contained in the weak features between 1.75 and 2.10 Å , and consequently this is the region where the two spectra differ significantly. It is important to note how weak the

features in this region are; it is only by taking the difference between the $i(Q)$ functions and obtaining a real space correlation function by Fourier transformation that information about the Ti environment can accurately be obtained. Figure 2(b) illustrates this point well. The Ti-O correlation clearly contains two distances at ~ 1.8 and $\sim 2.0\text{ Å}$, with the latter seen as a distinct, partially resolved shoulder. This is the first direct, unequivocal observation of two Ti-O distances in this type of material.

The structural parameters obtained from simulation of the difference interference functions are presented in Table 2 (the fit parameters associated with the silica host network are not included here; they are as would be expected for a sol-gel silica glass and add nothing to the discussion of the Ti environment *per se*). Figure 3 shows the MAS NMR ^{17}O spectra after heat treatment to various temperatures.

This composition exhibits very interesting structural behaviour with significant changes occurring throughout the temperature range studied. The titanium site in the sample heated to 250°C is characterised by a very broad correlation due to Ti-O bonding. The results in Table 2 again suggest at least two distinct Ti-O distances. The neutron difference data can be simulated by an average titanium nearest neighbour environment of four oxygen atoms at a distance of 1.89 Å and two oxygen atoms at a longer distance of 2.11 Å . This type of distorted octahedral environment is observed in the mineral ramsayite which has four shorter Ti-O bond lengths in the range $1.82\text{--}1.96\text{ Å}$ and two in the range $2.14\text{--}2.18\text{ Å}$.⁽³¹⁾ The origin of this distorted TiO_6 site in this sample appears to be the desire of Ti^{IV} to expand its coordination sphere above four by forming longer non-network forming bonds to H_2O and OH^- ligands. Further evidence that the longer Ti-O distances are indeed due to weaker bonds to H_2O and OH^- ligands comes from a previous high temperature XANES study⁽¹⁷⁾ that demonstrated the abundance of reversible $\text{TiO}_6 \leftrightarrow \text{TiO}_4$ sites in the structure of samples of this composition.

After heating to 750°C , the titanium environment in the sample becomes more well defined as can be witnessed by the much narrower Ti-O correlation: the parameters derived from the simulation analysis of this feature given in Table 2 indicate that two Ti-O distances are present, a short distance at 1.81 Å due to titanium tetrahedrally substituted within the silica network and a longer distance at 1.95 Å which is very close to the average Ti-O bond length determined from the mineral anatase (one of the crystalline forms of TiO_2 that has a structure consisting of TiO_6

Table 2. Structural parameters for the Ti-O correlations obtained from the simulation of the single difference correlation functions, $T_{\text{Ti-X}}(r)$. Each $T_{\text{Ti-X}}(r)$ was derived from the difference between the interference functions from the ^{46}Ti and ^{48}Ti enriched samples*

Sample	Correlation	$R/\text{Å} \pm 0.01\text{ Å}$	$N/\text{atoms} \pm 20\%$	$\sigma/\text{Å} \pm 0.01\text{ Å}$
$(\text{TiO}_2)_{0.18}(\text{SiO}_2)_{0.82}$	Ti-O	1.89	3.6	0.084
250°C	Ti-O	2.11	1.5	0.052
$(\text{TiO}_2)_{0.18}(\text{SiO}_2)_{0.82}$	Ti-O	1.84	3.0	0.060
500°C	Ti-O	2.02	1.4	0.060
$(\text{TiO}_2)_{0.18}(\text{SiO}_2)_{0.82}$	Ti-O	1.81	2.4	0.033
750°C	Ti-O	1.95	1.7	0.061

* R , N and σ represent the atomic separation, coordination number and disorder factor, respectively

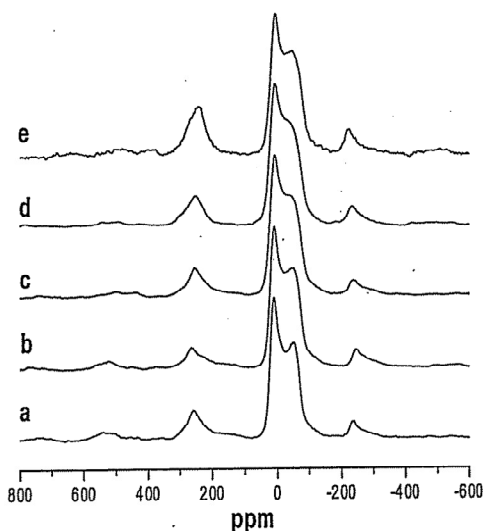


Figure 3. ^{17}O MAS NMR from the $(\text{TiO}_2)_{0.18}(\text{SiO}_2)_{0.82}$ samples after various heat treatment: (a) unheated, (b) 120°C , (c) 250°C , (d) 500°C and (e) 750°C

octahedra).⁽³²⁾ The average Ti-O coordination number determined at this temperature of heat treatment is close to four, suggesting that the majority of titanium in this sample is substituted within the silica network with a minority species present in a TiO_6 environment similar to that found in anatase. Indeed, the 750°C sample containing natural titanium exhibited very weak Bragg peaks in the $i(Q)$ data, the positions of which corresponded to those expected for anatase. Hence, it seems that at least some of the TiO_6 present in the samples heated to 750°C is in the form of phase separated TiO_2 which is on the point of crystallisation at this temperature.

At the intermediate temperature of heat treatment, the Ti-O environment is consistent with a mixture of TiO_4 sites and unstable, distorted TiO_6 sites. There is an

overall decrease in average Ti-O coordination number and associated decrease in the average Ti-O distance as the temperature of the heat treatment is increased. These changes are consistent with the conversion of TiO_4 sites to TiO_6 sites as a function of temperature, and agree well with the results of previous structural studies using XRD, and ^{29}Si MAS-NMR, XANES and EXAFS.^(16,33,34)

The ^{17}O NMR MAS spectra in Figure 3 again show a strong signal from the second-order quadrupole lineshape at ~ 0 ppm from Si-O-Si, and the Ti-O-Si peak at ~ 270 ppm. There is a small but nevertheless distinct peak at ~ 550 ppm corresponding to Ti-O-Ti, probably as OTi_3 .⁽²⁸⁾ The use of ^{17}O NMR therefore helps unequivocally to show that a very small amount of phase separation is occurring. As well as agreeing with the results from the NDIS analysis, these NMR results confirm that the $(\text{TiO}_2)_{0.18}(\text{SiO}_2)_{0.82}$ composition is indeed on the limit of solubility of TiO_2 in sol-gel silica.^(16,35)

Calcium-silica

The $i(Q)$ of the ^{nat}Ca and ^{44}Ca -enriched $(\text{CaO})_{0.3}(\text{SiO}_2)_{0.7}$ samples are shown in Figure 4, together with the corresponding weighted difference between the two. The structural parameters derived from fitting to both the original and to the difference function are provided in Table 3.

The parameters obtained for Si-O and O-O are as one would expect for porous sol-gel derived silica⁽³⁴⁾ and this lends confidence to the fitting of the other correlations observed. In a fully condensed silica network the O-O coordination number would be six, in these materials it is reduced to ~ 4.6 due to the presence of nonbridging oxygen atoms (NBO) which are abundant in high surface area materials. It is important also to note that the parameters obtained from the fit to the difference correlation function, $t_{\text{Ca-X}}(r)$, may be carried over to the fitting of the original datasets unchanged:

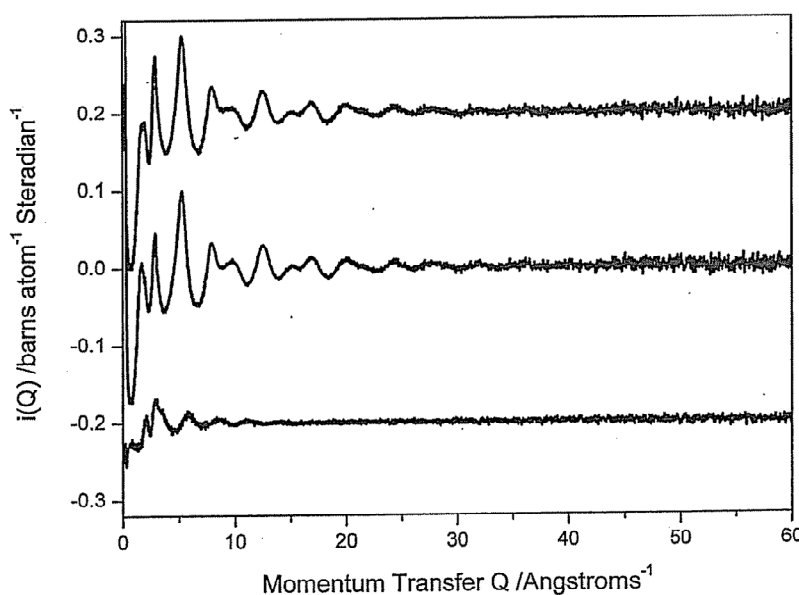


Figure 4. $i(Q)$ data for ^{nat}Ca (top) and ^{44}Ca (middle) $(\text{CaO})_{0.3}(\text{SiO}_2)_{0.7}$ and difference between $i(Q)$ functions from the ^{44}Ca and ^{nat}Ca samples. ^{nat}Ca and difference have been offset by $+0.2$ and -0.2 , respectively, for clarity

Table 3. Fitting parameters obtained from simulation of neutron diffraction data

Correlation	$R/A (\pm 0.01)$	$N_{\text{atoms}} (\pm 0.25)$	$\sigma/A \pm 0.01$
H-H	1.28	1.02	0.05
Si-O	1.61	3.8	0.05
Si-H	2.20	0.7	0.15
Ca-O	2.32	2.3	0.08
Ca-O	2.51	1.65	0.07
O-O	2.64	4.64	0.09
Ca-O	2.75	1.05	0.08
Ca-H	2.95	0.6	0.08

we take this as further evidence that the fits generated to $t_{\text{Ca-X}}(r)$ are robust.

The fit parameters obtained uniquely from the NDIS results show clearly that the Ca-O environment actually consists of distinct, but partially overlapping, correlation shells centred at 2.3, 2.5 and 2.75 Å. This is the first time a Ca-O environment of this complexity has been discerned in the context of contemporary bioactive glass materials: it is a key observation given the central role that Ca dissolution plays in the material's ability to promote bone growth. It is helpful at this point to draw comparisons with crystalline calcium silicate materials where Ca-O distances ranging from 2.3–2.8 Å have been observed, indicating that the values obtained here are certainly physically reasonable *per se*. In theory it should be possible to extract information from the NDIS data relating to higher correlations such as those from Ca-Si and Ca-Ca. However in practice, even using this method, the residual overlap between the large range of possible correlations above ~3 Å renders this unreliable as a quantitative exercise. What the NDIS results do offer is the uniquely detailed quantitative data required for computer simulation studies of bioactive glasses, and in particular towards the full understanding of the Ca dissolution and subsequent mineral deposition processes.

Conclusions

The (TiO₂)_{0.18}(SiO₂)_{0.82} samples exhibit the presence of two titanium environments at low temperature, the tetrahedrally substituted site and the distorted octahedral site formed when the titanium forms two extra bonds to OH⁻ ligands. Heating the sample to higher temperature converts some of the distorted octahedral sites to tetrahedral sites whilst the remainder becomes less distorted and more similar to the titanium site in anatase. A small amount of phase separation of TiO₂ is confirmed by both the neutron diffraction and the ¹⁷O MAS NMR. These results confirm that this composition is indeed on the limit of solubility of TiO₂ in sol-gel derived silica.

We have for the first time directly observed three Ca-O distances in a bioactive (CaO)_x(SiO₂)_{1-x} sol-gel glass and quantified their respective contributions to the bonding of Ca within the silica network. The data obtained point to a complex calcium environment in which the calcium is loosely bound at the surface of the network. This data provides a direct atomic scale explanation for the empirical observation that calcium loss from these materials is facile and can be achieved by simple ion exchange with body fluid.

It is only by such a detailed knowledge of the sites of importance in materials that systematic improvements in their application to tissue engineering can be achieved.

Acknowledgements

We thank the EPSRC for funding this work under awards GR/N64151, GR/N64267 and GR/R57492, and the CCLRC and its staff for their provision of synchrotron x-ray and pulsed neutron facilities. LJS acknowledges the support of the University of Kent School of Physical Science's Hyatt-Wolf fund for her studentship. We are grateful to V. Fitzgerald for her help in the collection of the neutron data.

References

1. Brinker, C. J. & Scherer, G. W. *Sol-Gel Science: The Physics and Chemistry of Sol-Gel Processing*, Academic, San Diego, 1990.
2. Schultz, P. C. & Smyth, H. T. In *Amorphous Materials*. Edited by R. W. Douglas & B. Ellis, Wiley, London, 1970, p. 453.
3. Davis, R. J. & Liu, Z. *Chem. Mater.*, 1997, 9, 2311.
4. Imamura, S., Nakai, T., Kanai, H. & Ito, T. *J. Chem. Soc. Faraday Trans.*, 1995, 91, 1261.
5. Beck, C., Mallat, T., Bürgi, T. & Baiker, A. *J. Catal.*, 2001, 204, 428.
6. *Introduction to Bioceramics*. Edited by L. L. Hench & J. Wilson, World Scientific, Singapore, 1993.
7. Hench, L. L. *Biomaterials*, 1998, 19, 1419.
8. Li, R., Clark, A. E. & Hench, L. L. *Chemical Processing of Advanced Materials*. Edited by L. L. Hench & J. K. West, Wiley, New York, 1992, p. 627.
9. Pereira, M. M., Clark, A. E. & Hench, L. L. *J. Mater. Synth. Proc.*, 1994, 2, 189.
10. Saravanapavan, P., Jones, J. R., Pryce, R. S. & Hench, L. L. *J. Biomed Mater. Res.*, 2003, 66A, 110.
11. Saravanapavan, P., Verrier, S., Jones, J. R., Beilby, R., Shirliff, V. J., Hench, L. L. & Polak, J. M. *Bio-Medical Materials and Engineering*, 2004, in press.
12. Dirken, P. J., Smith, M. E. & Whitfield, H. J. *J. Phys. Chem.*, 1995, 99, 395.
13. Anderson, R., Mountjoy, G., Smith, M. E. & Newport, R. J. *J. Non-Cryst. Solids*, 1998, 234, 72.
14. Rigden, J. S., Walters, J. K., Dirken, P. J., Smith, M. E., Bushnell-Wye, G., Howells, W. S. & Newport, R. J. *J. Phys. Condens. Matter*, 1997, 9, 4001.
15. Farges, F., Brown, G. E. & Rehr, J. J. *J. Phys. Rev. B*, 1997, 56, 1809.
16. Mountjoy, G., Pickup, D. M., Wallidge, G. W., Anderson, R., Cole, J. M., Newport, R. J. & Smith, M. E. *Chem. Mater.*, 1999, 11, 1253.
17. Mountjoy, G., Pickup, D. M., Wallidge, G. W., Cole, J. M., Newport, R. J. & Smith, M. E. *Chem. Phys. Lett.*, 1999, 304, 150.
18. Grunwaldt, J.-D., Beck, C., Stark, W., Hagen, A. & Baiker, A. *J. Phys. Chem. Chem. Phys.*, 2002, 4, 3514.
19. Sowrey, F. E., Skipper, L. J., Pickup, D. M., Drake, K. O., Lin, Z., Smith, M. E. & Newport, R. J. *J. Phys. Chem. Chem. Phys.*, 2004, 6, 188.
20. Skipper, L. J., Sowrey, F. E., Pickup, D. M., Fitzgerald, V., Rashid, R., Drake, K. O., Lin, Z., Saravanapavan, P., Hench, L. L., Smith, M. E. & Newport, R. J. *J. Biomed. Mater. Res.*, 2004, 70A, 354.
21. Holland, M. A., Pickup, D. M., Mountjoy, G., Tsang, S. C. E., Wallidge, G. W., Smith, M. E. & Newport, R. J. *J. Mater. Chem.*, 2000, 10, 2495.
22. Saravanapavan, P. & Hench, L. L. *J. Biomed. Mater. Res.*, 2001, 54, 608.
23. Saravanapavan, P. & Hench, L. L. *J. Non-Cryst. Solids*, 2003, 318, 1.
24. Cormier, L., Gaskell, P. H., Calas, G. & Soper, A. K. *J. Phys. Rev. B*, 1998, 58, 11322.
25. Hannon, A. C., Howells, W. S. & Soper, A. K. In *Proc. Second Workshop on Neutron Scattering Data Analysis*, 1990, IoP Conf. Series, 107. Edited by M. W. Johnson, Institute of Physics, Bristol, p. 193.
26. Yarker, C. A., Johnson, P. A. V., Wright, A. C., Wong, J., Gregor, R. B., Lytle, F. W. & Sinclair, R. N. *J. Non-Cryst. Solids*, 1986, 79, 117.
27. Gaskell, P. H. In *Materials Science and Technology*. Edited by J. Zrzycky, VCH, Weinheim, 1991, 9, p. 175.
28. MacKenzie, K. J. D. & Smith, M. E. *Multinuclear Solid State NMR of Inorganic Materials*. Pergamon Press, Oxford, 2002.
29. Gunawidjaja, P. N., Holland, M. A., Mountjoy, G., Pickup, D. M., Newport, R. J. & Smith, M. E. *Solid State NMR*, 2003, 23, 88.
30. Gervais, C., Babonneau, F. & Smith, M. E. *J. Phys. Chem. B*, 2001, 105, 1971.
31. Fletcher, D. A., McMeeking, R. F. & Parkin, D. J. from *The United Kingdom Chemical Database Service, Chem. Inf. Comput. Sci.*, 1996, 36, 746.
32. Burdett, J. K., Hughbanks, T., Miller, G. J., Richardson, J. W. & Smith, J. V. *J. Am. Chem. Soc.*, 1987, 109, 3639.
33. Pickup, D. M., Mountjoy, G., Wallidge, G. W., Anderson, R., Cole, J. M., Newport, R. J. & Smith, M. E. *J. Mater. Chem.*, 1999, 9, 1299.
34. Pickup, D. M., Mountjoy, G., Roberts, M. R., Wallidge, G. W., Newport, R. J. & Smith, M. E. *J. Phys. Condens. Matter*, 2000, 12, 3521.
35. Evans, D. L. *J. Non-Cryst. Solids*, 1982, 52, 115.